UNIVERSIDAD REGIONAL AMAZÓNICA IKIAM

FACULTAD DE CIENCIAS DE LA TIERRA Y AGUA

CARRERA DE GEOCIENCIAS

ANÁLISIS DE ESTABILIDAD EN EL ACCESO A LA CUEVA AGUAYACU, EN LA PROVINCIA DE NAPO, ECUADOR

Proyecto de investigación previo a la obtención del Título de:

INGENIERO EN GEOCIENCIAS

AUTOR

ANGEL RONALDO MEDINA ALTAMIRANO

Napo-Ecuador

2023

UNIVERSIDAD REGIONAL AMAZÓNICA IKIAM

FACULTAD DE CIENCIAS DE LA TIERRA Y AGUA

CARRERA DE GEOCIENCIAS

ANÁLISIS DE ESTABILIDAD EN EL ACCESO A LA CUEVA AGUAYACU, EN LA PROVINCIA DE NAPO, ECUADOR

Proyecto de investigación previo a la obtención del Título de:

INGENIERO EN GEOCIENCIAS

AUTOR: ANGEL RONALDO MEDINA ALTAMIRANO

TUTOR: PhD. JORGE RONNY ESPÍN CAMPOS

Napo-Ecuador

2023

DECLARACION DE DERECHO DE AUTOR, AUTENTICIDAD Y RESPONSABILIDAD

Yo, Angel Ronaldo Medina Altamirano con documento de identidad N° 1600527871, declaro que los resultados obtenidos en la investigación que presento en este documento final, previo a la obtención del título Ingeniero en Geociencias son absolutamente inéditos, originales, auténticos y personales.

En virtud de lo cual, el contenido, criterios, opiniones, resultados, análisis, interpretaciones, conclusiones, recomendaciones y todos los demás aspectos vertidos en la presente investigación son de mi autoría y de mi absoluta responsabilidad.

Tena, 16 de marzo de 2023

Firma:

_____

Angel Ronaldo Medina Altamirano

1600527871

CERTIFICADO DE DIRECCIÓN DE TRABAJO DE INTEGRACIÓN CURRICULAR

Certifico que el trabajo de integración curricular titulado: “Análisis de estabilidad en el acceso a la cueva Aguayacu, en la provincia de Napo, Ecuador”, en la modalidad de: artículo original, fue realizado por: Angel Ronaldo Medina Altamirano

El mismo ha sido revisado en su totalidad y analizado por la herramienta de verificación de similitud de contenido; por lo tanto, cumple con los requisitos teóricos, científicos, técnicos, metodológicos y legales establecidos por la Universidad Regional Amazónica Ikiam, para su entrega y defensa.

Tena, 16 de marzo de 2023

Firma:

_____

Jorge Ronny Espín Campos

C.I. 1600488207

AUTORIZACION DE PUBLICACION EN EL REPOSITORIO INSTITUCIONAL

Yo, Angel Ronaldo Medina Altamirano, con documento de identidad N° 1600527871, en calidad de autor/a y titular de los derechos morales y patrimoniales del trabajo de titulación: “Análisis de estabilidad en el acceso a la cueva Aguayacu, en la provincia de Napo, Ecuador”, de conformidad con el Art. 114 del CÒDIGO ÒRGANICO DE LA ECONOMÍA SOCIAL DE LOS CONOCIMIENTOS, CREATIVIDAD E INNOVACIÒN, reconozco a favor de la Universidad Regional Amazónica Ikiam una licencia gratuita, intransferible y no exclusiva para el uso no comercial de la obra, con fines estrictamente académicos.

Así mismo autorizo a la Universidad Regional Amazónica Ikiam para que realice la publicación de este trabajo de titulación en el Repositorio Institucional de conformidad a lo dispuesto en el Art. 144 de la Ley Orgánica de Educación superior.

Tena,16 de marzo de 2023

Firma

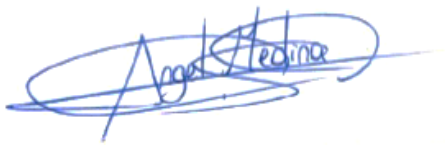

Angel Ronaldo Medina Altamirano

160052787

DEDICATORIA

Este trabajo está dedicado a mis dos angelitos en el cielo como lo es mi padre y mi abuela materna. También, dedico a los jóvenes amazónicos que desean ser parte de la comunidad científica.

AGRADECIMIENTO

En primer lugar, agradezco a mis tres tutores por el apoyo incondicional y las palabras de aliento para finalizar la investigación. Consiguientemente, doy relevancia a la educación recibida por todos los docentes pertenecientes a la Universidad ya que gracias a ellos fui formado de una manera excepcional. Finalmente, doy gracias a Dios por las bendiciones y por las personas que siempre estuvieron a mi lado que a pesar de las adversidades me supieron apoyar. En el cielo tengo a dos personas muy especiales que me guiaron en su paso por la tierra, mi padre y mi abuelita materna, este escalón profesional en mi vida va para ellos.

TABLA DE CONTENIDO

ÍNDICE DE TABLAS

ÍNDICE DE FIGURAS

RESUMEN

La provincia de Napo, en la lluviosa región amazónica de Ecuador, cuenta con una geodiversidad de cuevas kársticas muy visitadas por turistas de todo el mundo. La probabilidad de derrumbes y colapsos de las cuevas kársticas es una preocupación que afecta a las actividades turísticas y culturales que se desarrollan en estos espacios. El acceso a la cueva Aguayacu, ubicada a 14 km de la capital provincial de Napo, se caracteriza por la presencia de desprendimientos de bloques masivos de caliza, caliza fosilífera y lutita. Por ello, en esta investigación se realizó un análisis de estabilidad en la entrada de la cueva. Se establecieron cinco estaciones geomecánicas para detallar la ubicación, la litología, el grado de meteorización y los parámetros geotécnicos de las discontinuidades, como la resistencia a la compresión uniaxial, el espaciado, la apertura, la rugosidad, el relleno y el nivel freático. Con estos datos se determinaron las clasificaciones Rock Mass Rating (RMR) y Geological Strength Index (GSI). Posteriormente, se realizó un Análisis de Elementos Finitos utilizando el criterio de fallo de Hoek y Brown en el software RS2 para determinar el Factor de Reducción de Resistencia (SRF) y los desplazamientos máximos de las zonas inestables. Obtuvimos valores de GSI de 60-65 para la capa de esquisto, 68-73 para la caliza fosilífera y 77-85 para la caliza masiva, lo que indica una buena calidad de la roca. Además, determinamos una zona crítica con un SRF de 0,89, sin embargo, toda la sección de la entrada de la cueva no puede declararse inestable. El análisis de elementos finitos obtuvo desplazamientos máximos entre 0,030 y 0,037 m. Estos desplazamientos son mínimos en comparación con otras investigaciones. La cueva es estable a nivel de sección con un valor SRF > 2,21. Además, la calidad de la roca a partir de las clasificaciones geomecánicas indica que la cueva no está sujeta a desequilibrios de tracción que puedan desencadenar inestabilidad. No obstante, debe prestarse atención a las paredes de la cueva en las que se obtuvo un SRF < 1, que coincide con la zona de desprendimientos de placas de roca esquistosa. Se aconseja a los guías turísticos que establezcan un itinerario alejado de las zonas de desprendimiento de rocas inestables.

Palabras clave: Elementos Finitos, Clasificación del macizo rocoso (RMR), Índice de fuerza geológica (GSI), RS2, Factor de reducción de fuerza (SRF).

ABSTRACT

Napo province has a geodiversity of karst caves, which are visited by a large number of tourists annually. In general, underground spaces of karst origin exhibit stability at a global level, however, they can present collapses, rockfalls, and various types of geological hazards associated with their nature. The geographical location of the study area is characterized by sedimentary shale and limestone rocks, heavy rainfall, and significant development of organic soil. The present study focused on analyzing the stability of the Aguayacu cave using finite elements and a non-linear failure criterion, based on five geomechanical classifications RMR and GSI. The analyzed results were based on the strength reduction factor and the maximum displacements. The walls of the cave corresponding to the shale rock layer presented SRF<1 values and displacements <0.037 m. The roof of the cave presented SRF>2.2 values and displacements <0.025. It was concluded that at the section level, the cave is stable. Additionally, tabular blocks were evidenced on the floor, which is the main hazard.

Keywords: Finite Elements, Rock Mass Rating (RMR), Geological Strength Index (GSI), RS2, Strenght Reduction Factor (SRF).

INTRODUCTION

Geodiversity preexistent in Ecuador benefited the province of Napo, in which there is a variety of caverns, caves, and grottoes that, thanks to different tectonic-structural, geomorphological processes, among others, have given rise to its variability (Benito et al., 2009; Das, 2001). In Ecuador, the informative activities on speleology have been few or almost non-existent, therefore, finding scientific information on these topics is very difficult. The Geopark Project Napo Sumaco developed a geotourism inventory of the natural cavities belonging to the province of Napo, where a compendium of speleological research was carried out at the provincial level, in the fields of geology, geomorphology, biology, hydrology, local manifestations and tourist resources (Sánchez Cortez, 2017).

The rocks present in this eastern sector favoured the formation of these natural cavities, in addition, the high rainfall typical of the Ecuadorian Amazon helps to dissolve the soluble rocks, generating these formations. These natural cavities are part of the karstic terrain of the Napo formation present in the area, composed chiefly of carbonate rocks (Sánchez Cortez et al., 2017). In turn, the water present inside the caves is the element that creates the caverns, but in turn, is to blame for their collapse and subsequent disappearance, if there is a large amount of water in the cavity, over time it will tend to collapse, being the case of the Amazonian caves. The study area is located within the territory belonging to the Napo Sumaco Aspiring UNESCO Geopark (Vera et al., 2023).

Most of the caves have been sites that the oldest human beings have used as a refuge or as ceremonial temples, but they are currently used as a tourist attraction (Jordá-Bordehore et al., 2016). Some small caverns may suffer collapses or landslides in areas where the rock has high degrees of fracture.

The present investigation carried out a stability analysis in the Aguayacu cavern access, through a finite element analysis and a geomechanical classification.

Study area

Aguayacu community is located northeast of the city of Archidona, 14 km from the city of Tena, shown in figure 1. Archidona has a warm humid climate, with rainfall that varies between 4,000 and 5,000 mm per year, its minimum altitude is 613 meters above sea level and its maximum is 4,294 meters above sea level (Guacamayos range), has an average temperature of 24 ° C, and an atmospheric pressure of 712 mm. The average annual humidity of Archidona is 80%, with maximum values at the time of greatest precipitation during the months of June and July (GADMA, 2014).

The cave system of the Aguayacu Community is managed by the Aguayacu Tourist Association. Upon reaching the community, it is necessary to contact the leaders, who will give you all the information on the places that can be visited in the sector. Afterward, there will be walks through established trails that will allow you to reach the caves (Sánchez Cortez, 2017).

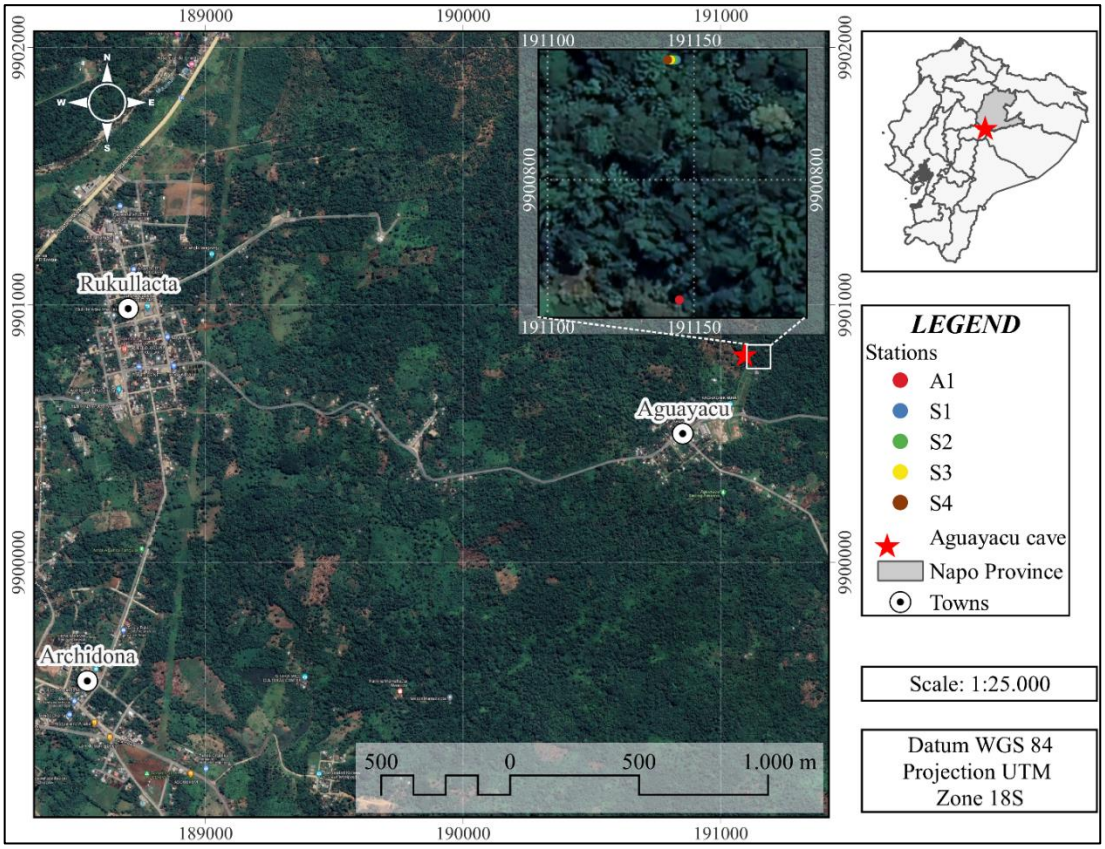

Figure 1: Cave location map.
Elaborated by: Angel Medina
The red star indicates access to the cavern, in addition, the red, blue, green, yellow, and brown points show the location of the stations. The Rukullacta and Aguayacu communities have been indicated as references.

GEOLOGICAL SETTINGS

Caves by dissolution are formed from the dissolution processes of the rock in conjunction with groundwater. For the aforementioned process, two elements are required, the first is that the rock is soluble and the second is that the water is chemically active.

As Figure 2 shows us, the Napo formation is the one that dominates in the study area, in which shale, black limestone, marine limestone rich in organic matter, and sandstone can be found (Baby et al., 2004). The Napo formation belongs to the Cretaceous geological period with an approximate age of 70 to 90 million years (Baby et al., 2004; Shanmugam et al., 2000). The Lushian River and the presence of two faults near the cave are appreciated, among them are the Porotoyacu fault and a little further away the Jondachi River fault. The Napo Formation is a calcareous unit, characterized by the presence of abundant fossil fauna and a high presence of limestone in the middle part, and the rocks of this same formation exist in the Misahuallí River and the Hollín River to the north. According to (Vallejo et al., 2002), the Napo formation was subdivided into four different formations, (1) Napo Basal Formation, which includes a calcareous member at the base, a lutaceous member called Lutita Basal, and an oil-bearing member; (2) Lower Napo Formation, also has a calcareous member in the base, shales in the middle section and an oil interval between calcareous and sandy in the upper part; (3) Middle Napo Formation, includes shallow carbonate platform deposits, which differ in their faunal diversity and the presence of sandstone; (4) Upper Napo Formation, composed of alternate shale, limestone, and sandstone. This formation is characterized by a variety of fossil fauna and organic matter. In addition, this research was carried out in the middle and upper part of the Napo formation (Baby et al., 2004).

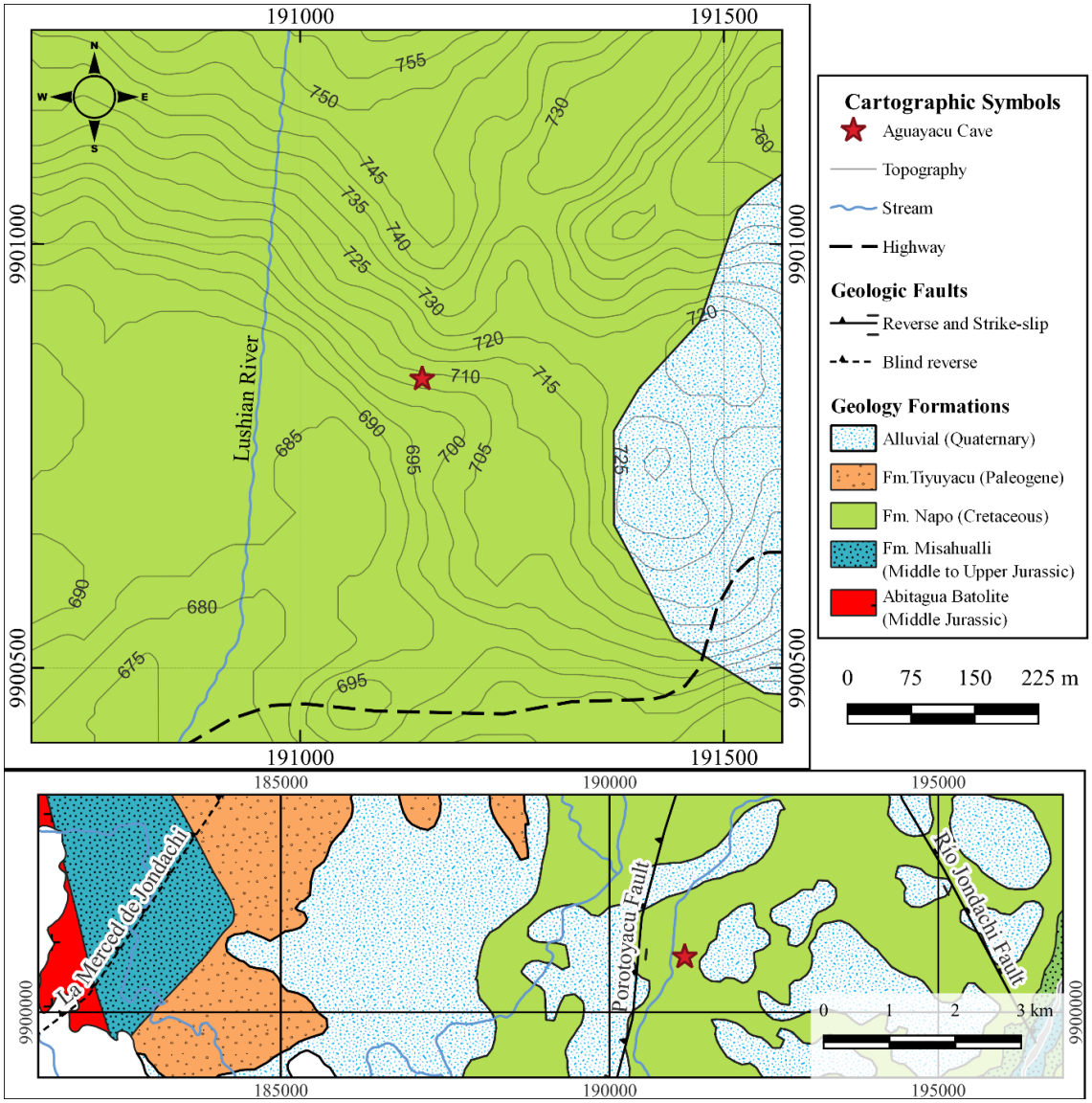

Figure 2: Geological map of the study area.
Elaborated by: Angel Medina
In the upper left part, the topographic map of the area is denoted, in addition to the Lushian River and the main road that leads to the cave. In the lower part, the geological faults found in the place are observed, among them are the Porotoyacu fault, which is a Reverse and Strike-slip fault, also, the Jondachi river fault, and finally La Merced de Jondachi fault, which is a Blind reverse fault. On the other hand, Napo formation is predominant in the map with green coloration, and an alluvial deposit is also observed near to the cave.

MATERIALS AND METHODS

In the months of February, March and April 2022, an in situ geological and geotechnical characterization of the access to the Aguayacu cave was carried out. At this site, information was collected from 5 geomechanical stations identified as S1, S2, S3, S4 and A1, along the study area, as shown in Figure 1. These stations were selected based on lithological and structural criteria present in the rock mass. Stations S1, S2, S3 and A1 were installed on the outside of the cavern, while station S4 was installed inside the cavern. Table 1 shows the coordinates, lithology and moisture conditions of the identified stations. In addition, the degree of weathering of the rocks and what the weather was like that day are shown. Most of the day when the data were taken there was no water present, but at other stations the water inflow was higher as there was a small stream. The geomechanical survey conducted at S4 was more specific as it was inside the cavern, Figure 4.

Table 1: Coordinates, lithology and climate description for the area of interest.

Station ID	Longitude	Latitude	Lithological Description	Weathering degree (ISRM, 1981)	Weather in situ
S1	0191144	9900841	Sedimentary limestone type, massive.	Moderately weathered	Dry (Signs of water)
S2	0191143	9900841	Sedimentary limestone type, massive.	Highly weathered	Dry (Signs of water)
S3	0191142	9900841	Limestone types sedimentary, massive, near a water sink.	Moderately weathered	Dry
S4	0191143	9900841	Three types of rocks, massive limestone, black shale and fossiliferous limestone.	Highly weathered	For massive limestone there is a permanent water flow
A1	0191145	9900759	Massive Limestones and Black Shales.	Moderately weathered	Dripping in the outcrop area

Elaborated by: Angel Medina

Geomechanical classifications

Geomechanical stations were used in order to collect input parameters for the analysis of cavern stability by applying finite elements. Data was processed in order to obtain geomechanical classifications in terms of Rock Mass Rating (RMR) (Bieniawski, 1989) and Geological Strenght Index (GSI) (Hoek et al., 1998). The RMR was originally created for the execution of subway excavations, and have been used since 1970 until today. These methods are applied worldwide by professionals in rock mechanics, which allows the characterization, classification, and understanding of the properties of rock masses (Tomás et al., 2020). The GSI has been utilized in back-analysis of tunnels, karstic caves, slopes, and rock mass foundations (Alemdag et al., 2019).

The RMR is a classification system for rock masses that allows relating rock mass quality index to design parameters (strength and deformability) and tunnel support (Bieniawski, 1989). The RMR is based on 6 parameters: uniaxial strength of the rock matrix, fracture degree in terms of RQD, discontinuity spacing, joint conditions, hydrogeological conditions, orientation of discontinuities with respect to the cave structure (Bieniawski, 1989). The GSI classification is a system that is applied to rock masses by observation. The factors used by the GSI are rock mass structure, joint roughness and alteration (Vassilis, 2020). The quality scores in both RMR and GSI range from 0 to 100, where the value in RMR rating <20 means very bad quality and the 100 value means very good quality. Also, in GSI the value <10 means a foliated/laminated rock mass and the >90 is a rock intact or mass, as seen in Appendix A1.

Currently, these geomechanical classifications are still applied, in addition, research proposes their application in caverns or underground labours (Bastidas et al., 2022; Bhasin et al., 1995; Espín et al., 2022; Hoek, 2007; Sapigni et al., 2003).

Finite element analysis, failure criterion and input parameters

Finite element analysis is an automated engineering method that has made it possible to predict how a product will react to exposure to heat, fluids and vibrations, among other real-world physical effects. Technological advances have helped geotechnical engineering to rely on these methods to perform numerical simulations (Pandey et al., 2022). Finite elements are considered the most recent and comprehensive tool for evaluating stresses and strains (Herrera Mazuera, 2015). In our case, the RS2 program was used, which belongs to the rocscience package (Rocscience, 2022).

The failure criterion used for the numerical calculation was that of Hoek et al. (2002). For this criterion to work, several parameters are required, particularly the value of GSI. However, the value of GSI, being subjective and dependent on the specialist's criteria, is highly variable. For this reason, the RMR value was calculated as a means of verifying that the GSI value does not vary significantly with respect to the RMR. The other parameters required by the failure criterion correspond to the uniaxial compressive strength (UCS), constant (mi), disturbance factor (D). In order to obtain the geomechanical parameters in terms of cohesion and friction, the RocLab program was used (Rocscience, 2022).

The rebound values were obtained on the surface joint walls and the rock matrix using the Schmidt hammer. The rebound values were used to calculate the Uniaxial Compressive Strength (UCS), and in turn, the unit weight was determined through bibliographic references (González de Vallejo et al., 2002). The intact rock constant m_i is an important factor for the Hoek-Brown failure criterion (Hoek et al., 2000). This constant indicates the behavior of the intact rock. Traditionally, the constant m_i is determined by a laboratory triaxial test on rock cores with a diameter of 50 mm and a length of 100 mm, however, due to unfavorable time or budget conditions, it can be determined from tables based on the results of triaxial test performed on intact rock (Hoek et al., 2000).

Several factors such as heavy blast damage, lateral confinement or reduction of stress due to overburden can result in alterations to the rock mass. To take these alterations into account for the rock mass, the Hoek-Brown failure criterion considers including the disturbance factor D into the analysis. Thus, a disturbance rock mass is considered when D = 1, and an undisturbed rock mass when D = 0 (Hoek et al., 2002).

Deformation parameters E and v were calculated as follows. Young's Modulus is defined as the ratio of stress to strain. If the Young's modulus is low, the rock tends to be ductile, while if the Young's modulus is high, the rocks are brittle (Ma et al., 2016).

$$E_{rm}(MPa) = 100000\left(\frac{1-D/2}{1+e^{\left(\frac{75+25D-GSI}{11}\right)}}\right) \quad (1)$$

This equation shows the calculation of Young's Modulus. Where, D is the disturbance factor.

Poisson's Ratio is a measure of a material's ability to expand in directions perpendicular to the force applied to the material. This ratio is defined as the fraction of expansion divided by the fraction of compression. According to Vásárhelyi & Kovács (2017), there is a linear relationship, where it shows that as the quality of the rock mass decreases, the Poisson's ratio increases. Therefore, we use the equation 2 to compute the Poisson's ratio.

$$Vrm = -0.002GSI - 0.003mi + 0.457 \quad (2)$$

Where Vrm, Poisson's ratio of the intact rock.

This equation for calculating the Poisson value is found as a function of the GSI and the Hoek-Brown constant (mi).

Roclab software uses equation (1) to compute de Young´s modulus for each type of rock to be analysed, this result can be found in the Rock Mass Parameters section, see Appendix-Figures A4, A5, and A6. In turn, the Poisson's ratio was calculated using equation 2. The results are shown in Table 3.

Once the geomechanical parameters of all the layers have been obtained, a geological model of the cave is necessary for the RS2 program to perform the analysis. This model was obtained *in situ,* we took measurements of the height and width in order to generate a geometric model of the cave. This model was created in AutoCAD and the geologic model of the cave was imported into RS2. Then, the strata belonging to the study area were placed with their corresponding geomechanical properties, the water table was placed in the cave and an external force or load was applied, and finally, a mesh was applied.

The results correspond to the analyzed section shown in Figure 3. For the computation, it was considered that the biota exerts a superficially distributed load of 0.0079 MN/m^2, as well as the horizontal arrangement of three types of rocks.

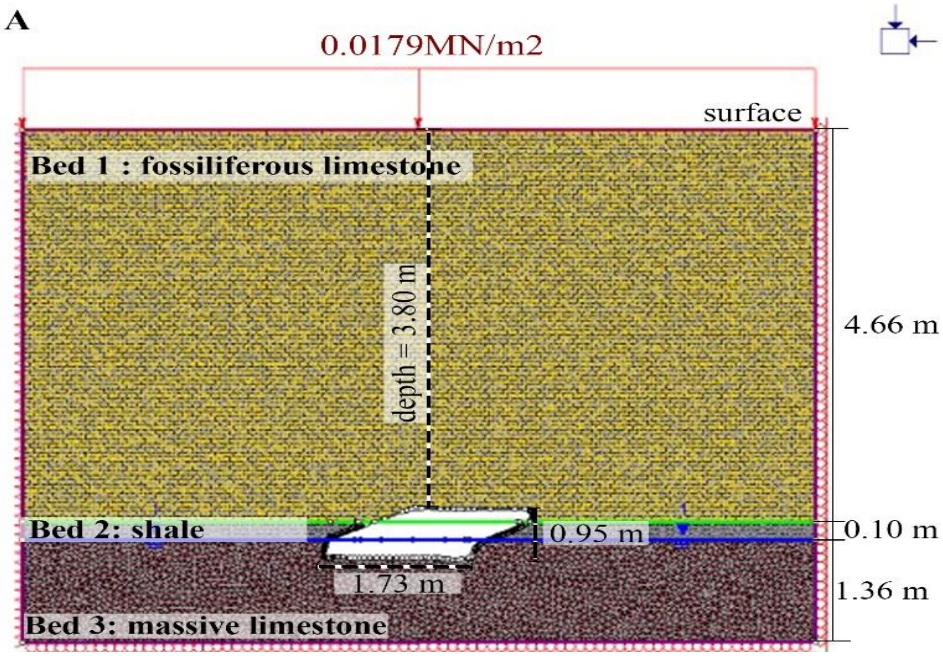

Figure 3: Detailed geometrical and geological model of the analysed section.
Elaborated by: Angel Medina

RESULTS

The parameters to compute the geomechanical classifications are shown in Table 3. In the Figure 4 shows the geomechanical stations where the geological and geotechnical data was collected.

Table 2: Geomechanical classification according to the value of RMR and GSI
Results of the evaluation of the rock mass geotechnical parameters to obtain the value of geomechanical classifications RMR and GSI.

Station ID	Plane type	Orientation	UCS	RQD	Spacing of discontinuiti	Persistence	Opening	Rugosity	Filling	Disturbance	Undergroun d water	RMR	GSI
			Puntuation										
S1	J1	216/86	2	20	10	2	0	5	2	3	7	49	77-85
	S0	143/45	2	20	10	2	0	5	0	1	7		
S2	J1	323/52	2	20	10	4	0	5	4	1	7	49	77-85
	J2	231/20	2	20	10	4	0	0	0	0	7		
	J3	24/74	2	20	15	4	0	0	2	1	7		

S3	J1	334/13	2	20	10	4	0	5	0	3	15	57	77-85
	S0	255/20	2	20	8	1	3	5	0	1	15		
S4	S0a (Fossiliferous limestone)	145/22	2	20	10	2	1	5	4	1	10	45	68-73
	S0b (Massive limestone)	235/5	2	20	10	4	0	0	0	0	0		77-85
A1	J1	295/80	2	20	10	4	0	5	4	1	4	50	77-85
	J2 (Shales)	320/85	0	20	10	4	1	5	0	1	7	48	60-65
	S_0	235/6	2	20	10	4	0	0	0	0	0	44	77-85

Elaborated by: Angel Medina

The calculated values for the GSI of the three types of rocks found in the cave were the following: Fossiliferous Limestone with a value of 68-73, Figure A1, Massive Limestone 77-85, Figure A2, and the Shales with a value of 60-65, Figure A3. In addition, Figure 5, shows the types of rocks found within station S4, which could be identified: A) Fossiliferous Limestone, B) Shale and C) Massive Limestone.

Figure 4: Geomechanical stations for this study and the outcrop near the cave are shown. Persons and geological hammer as scale.
Elaborated by: Angel Medina

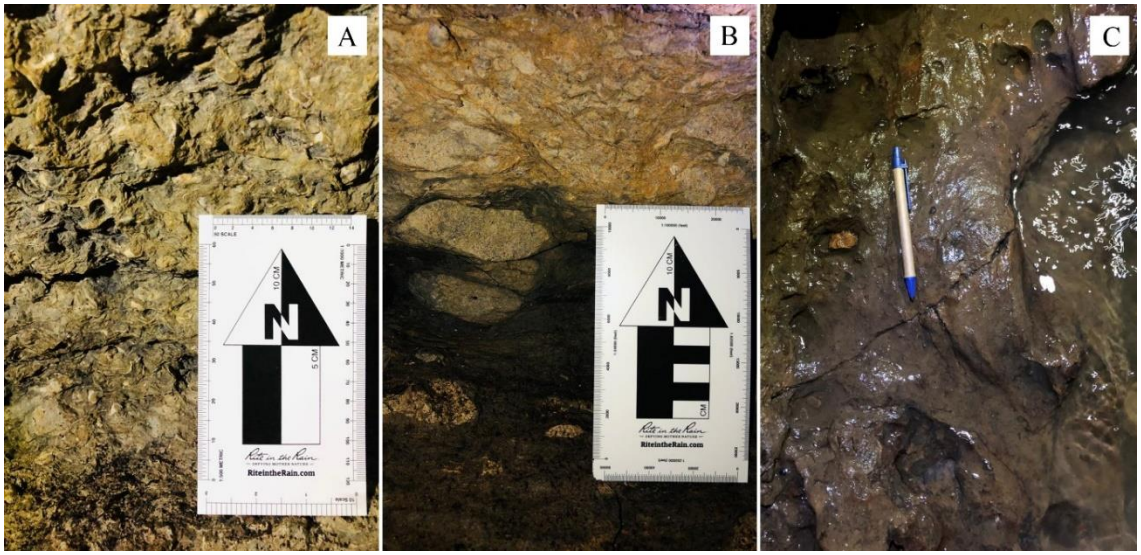

Figure 5: Types of rocks found inside the cave. A) Fossiliferous Limestone, B) Shale and C) Massive Limestone.
Elaborated by: Angel Medina

Table 4 corresponds to the input parameters used for the Strenght Reduction Factor calculation.

Table 3: Geomechanical parameters

Layer	Rock Mass	Unit Weight (MN/m3)	Uniaxial Compressive Strength (MPa)	Young's Modulus (MPa)	Poisson's Ratio	Friction Angle (deg)	Cohesion (MPa)
1	Fossiliferous limestone	0.024	11	10992.21	0.28	58.96	0.28
2	Shale	0.022	0.50	3354.75	0.31	34.79	0.01
3	Massive limestone	0.024	8	12245.25	0.27	56.48	0.29

Elaborated by: Angel Medina

Strenght reduction factor

Figure 6 shows the zones of total displacements along with the deformation vectors, whose direction points towards the boundaries of the cave. On the left wall of the cavern, the areas in red and orange denote the most critical zones that can be displaced, which show a maximum displacement of 0.030 m. This is the critical zone of displacements, where the deformation vectors stack up to a greater extent than in other areas. In the central or ceiling part of the cavern, the displacement ranges vary from 0.018 to 0.024 m. and are denoted in light green to yellow color. While the right and bottom walls of the cavern present maximum displacements of 0.0000132 m. and are denoted in bluish to cyan colors. The light blue horizontal line represents the position of the water table. We

determined a range of critical values from 0.030 m. to 0.037 m., which represents the layer-to-layer displacements in the Y axis. Furthermore, Figure 6 and Figure 7 indicates that the most critical area of displacements is located at the entrance of the cave, specially at the top.

Figure 7 indicates the zones of critical values for the Strength Reduction Factor (SRF). On the left wall of the cavern, the zone with the maximum critical SRF value of 0.89 is shown in yellow and orange. Values of SRF within the range of 2.21 to 3.47 are shown in greenish color on the ceiling and base of the cavern.

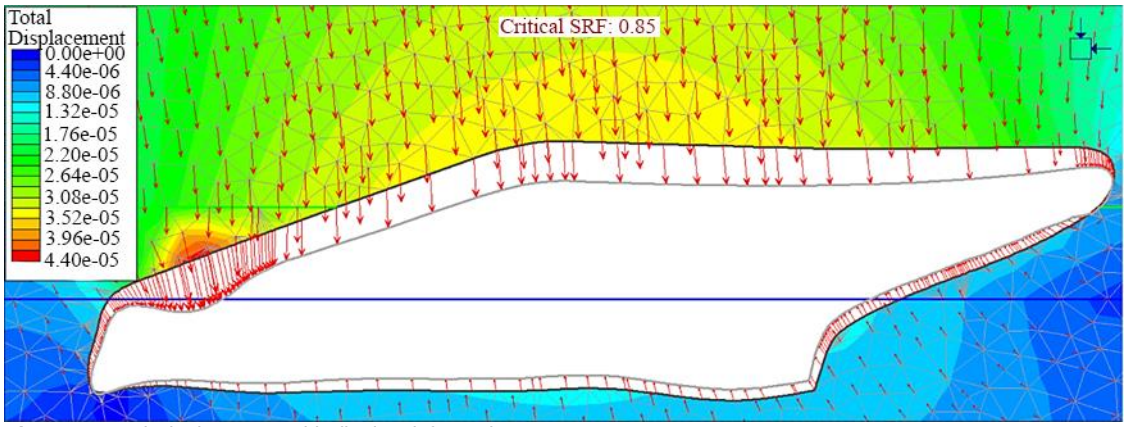

Figure 6: Total Displacement with display deformation vectors.
Elaborated by: Angel Medina

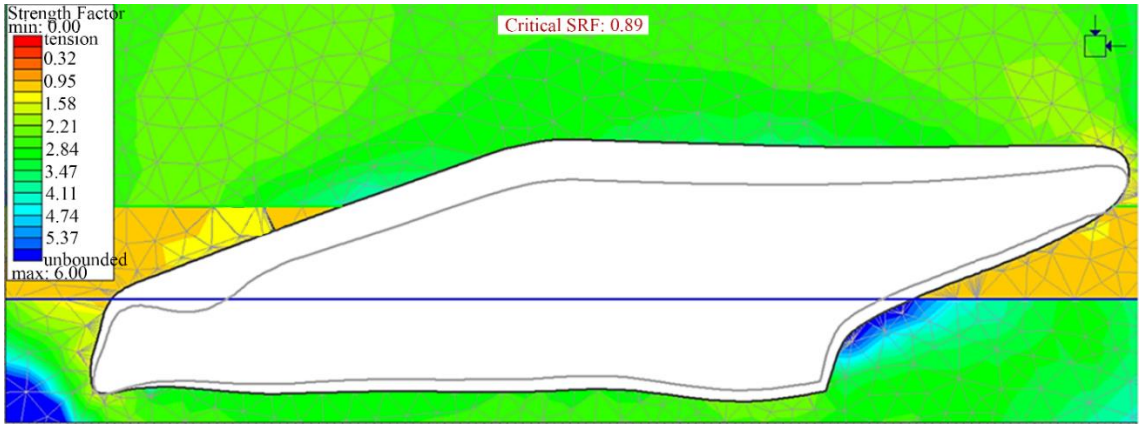

Figure 7: Finite element analysis of the access to the Aguayacu cave with safety factor and maximum shear stress distribution, also shows the deformed limit, the joints were excluded to avoid complexities in the calculation.
Elaborated by: Angel Medina

DISCUSSION

The geological and geotechnical characterization yielded an average RMR rating of 50 for the limestone layer, being a class III rock (medium quality). In turn, the RMR rating for the shale layer was 48, which is a class III rock (medium quality) (Bieniawski, 1989). According to Singh et al. (2019) the RMR ratings for shale layers ranges from 38.4 - 55.8, our results are within this range. RMR ratings for massive limestone range from 31 - 47 according to Shalabi et al. (2009), our RMR ratings assessment is slightly above this range. Waltham & Fookes (2005) mention that the quality of a karstic rock mass can be of Class II or good quality, with a Q index between 4 - 10 (Barton et al.,1974) and a RMR range from 40 - 60 based on Bieniawski (1989). Our RMR ratings for geomechanical stations are within this range.

Regarding the GSI index, ratings were obtained that fall into the category of good quality rock for shale layer (60 – 65 points), and very good quality for both fossiliferous limestone layer (68 – 73) and massive limestone layer (77 – 85). Marinos & Carter (2018), mention that the GSI ratings range for shales is between 15 – 25 points, due to their fine stratification similar to schistosity. Similarly, Marinos & Carter (2018) mention that when limestones are massive or arranged in thick layers, and are far from areas of disturbance by tectonics, it is expected that the GSI fracture index will range from intact to very blocky, as shown in Figure 3.

RQD values in the four geomechanical stations were above 90%, which means that the rock has a low degree of fracturing. That is because the average spacing of the joint sets is greater than 60 cm. In fact, in some areas of the limestone layer, the structure was intact without any visible discontinuity. However, this parameter does not include the orientation, filling, alteration, and other conditions of the discontinuities, therefore, it does not consider these surface characteristics that are important when evaluating the geomechanical behavior of the rock mass (González de Vallejo et al., 2002).

The range of UCS values for the massive limestone layer were 5.9 to 8 MPa. For the fossiliferous limestone layer, the UCS value was 11 MPa. While the shale layer is at 0.5 MPa. According to the ISRM (2015) classification of rock mass quality based on the UCS, geomechanical stations S1, S2, S3 and S4 were classified as low quality (UCS = 6 - 10 MPa), while station A1 was classified as medium quality (UCS = 20 - 60 MPa) (Sajid & Arif, 2015). Aydin & Basu (2005) mention that the surface condition of

discontinuities, such as roughness, joint degree, moisture content and sclerometer axis can reduce rebound value, and thus the UCS values.

The roughness of the discontinuity surfaces was categorized between undulating rough and staggered rough. During the fieldwork, we note that the surface roughness of massive and fossiliferous limestone layers increases depending on the degree of weathering. This indicates that the roughness categories found in this study correspond to highly weathered limestone rock samples. Similarly, Aydin & Basu (2005) point out that weathering is considered a conditioning factor for obtaining rebound values, since it generates micro-level changes in the structure of the rock mass. Thus, scattered rebound values are expected while increasing the degree of weathering (Aydin & Basu, 2005). In the 5 geomechanical stations, the presence of both dripping water and in constant flow and characteristic humidity of the cavern was evidenced. In addition, near station A1 (approximately 3 meters) there is a water sink which is flooded in rainy seasons. Sumner & Nel (2002), mention that the rebound values decrease non-linearly when the moisture content increases, and therefore the resistance of the lithologies under study. In addition, the tropical climate of the region is a factor that determines the stability of the wall cave, since it accelerates the process of dissolution and weathering in the Amazonian karstic system (Piccini & Mecchia, 2009).

We obtain a SRF value of 0.89, which is considered a low safety factor, considering that SRF values greater than 1 indicate a safe or stable zone (Pandey et al., 2022). It is important to note that the SRF value is only a general value (Hammah et al., 2005), this means that the SRF value of 0.89 cannot be assumed to be unstable for the entire section. This value of 0.89 corresponds specifically to the shale layer, this is consistent because the shale layer has the lowest resistant parameters compared to the other layers. We can even see that the roof has SRF values between 2.2 and 2.8, and that the values lower than 1 are actually concentrated in the walls. Based on the above, it can be deduced that the cavern would be globally stable. This result is consistent with the global stability analysis of the Humanti cavern (Yépez et al., 2022). It is important to mention that the lithology of the mentioned study is similar to the present investigation. In fact, the distance between study areas is 3 km.

However, where SRF values are less than 1, it could be understood as zones that are being affected by lithostatic stresses, chemical weathering, and that, due to their lithology susceptible to detachment in parallel planes, the material is detaching. In situ observations are faithful witnesses of the detachments.

From the results obtained in our study, Figure 6 indicates that the total average displacement of 0.025 m. Akgün & Koçkar (2004) report maximum displacements between 0.662 to 0.974 m in a man-made cavern in silty limestone. Nadimi et al. (2011) report displacements of 0.272 to 0.474 m in a cavern for a 132-meter-long powerhouse established in an area of dark and red shales. Spyridis et al. (2018) report displacements between 0.227 to 0.418 m for the excavation design of a tunnel for a light rail transit project in Ottawa. The tunnel is excavated over layers of shale and limestone with minimal coverage of a soil layer. Van Kien et al. (2022) determined maximum vertical and horizontal displacements of (-0.064) m and (0.147) m, respectively, in a large-scale underground cavern. Sari (2022) reports maximum displacements of 0.260 m at a depth of 5 m in storage caverns in soft tuff rock masses belonging to the Kavak formation in Turkey.

The displacements in the previous cited investigations are minimal, and in all of them, the underground space exhibits stability.

CONCLUSIONS AND RECOMMENDATIONS

The stability of the cavern is stable at section level, this is supported by the SRF values > 2.21 of the roof, and the small magnitude displacements obtained. Another aspect that indirectly informs about the stability is the quality of the rock mass obtained from the geomechanical classifications. Station A1 both in its RMR and GSI values show that the massif is of medium and good quality respectively. This is in agreement with the quality of the massif at stations S1, S2, S3 and S4. In addition, being a cavern where the subway space was formed naturally, the massif is not subjected to tensional imbalances, which contributes to the cavern maintaining its stability.

Specifically, attention should be paid to the walls of the cavern, since it was where SRF<1 values were obtained, coinciding with tabular plates, observed in situ drops of approximately 20 cm, which belong to the shale layer. However, this zone does not jeopardize the global stability because the shale layer has a thickness of not considerable dimensions and the orientation of the stratification plane is horizontal.

When the cavern is visited by tourists, the guides in charge of the tour should be in charge of marking the route, staying away from the walls of the cavern that show a

tendency to plate detachment. Monthly inspections are recommended in order to make an inventory of rockfall zones, which will help in defining the route.

REFERENCE

Akgün, H., & Koçkar, M. K. (2004). Design of anchorage and assessment of the stability of openings in silty, sandy limestone: A case study in Turkey. *International Journal of Rock Mechanics and Mining Sciences*, 41(1), 37–49. https://doi.org/10.1016/S1365-1609(03)00073-X

Alemdag, S., Zeybek, H. I., & Kulekci, G. (2019). Stability evaluation of the Gümüşhane-Akçakale cave by numerical analysis method. *Journal of Mountain Science*, 16(9), 2150–2158. https://doi.org/10.1007/s11629-019-5529-1

Aydin, A., & Basu, A. (2005). The Schmidt hammer in rock material characterization. *Engineering Geology*, 81(1), 1–14. https://doi.org/10.1016/J.ENGGEO.2005.06.006

Baby, P., Rivadeneira, M., & Barragán, R. (2004). Situación, morfología y deformación de la cuenca oriente. En *La cuenca Oriente: geología y petróleo: Vol. I* (p. 14).

Benito, A., Pérez, A., Magri, O., & Meza, P. (2009). Assessing regional geodiversity: the Iberian Peninsula. *Earth Surface Processes and Landforms*, 34(March), 613–628. https://doi.org/10.1002/esp

Bieniawski, Z. T. (1989). Engineering Rock Mass Classifications: A Complete Manual for Engineers and Geologists in Mining, Civil and Petroleum Engineering. Jhon Wiley & Sons.

GADMA. (2014). Plan De Desarollo Y Ordenamiento Territorial Archidona. *Dirección de Planificación del GADM Archidona*, 1–174.

González de Vallejo, Luis I., Ferrer, M., Ortuño, L., & Oteo, C. (2002). *Ingeniería Geológica*. PEARSON EDUCATION.

Hammah, R. E., Yacoub, T. E., Corkum, B. C., & Curran, J. H. (2005). The shear strength reduction method for the generalized Hoek-Brown criterion. *Proc. American Rock Mechanics Association - 40th US Rock Mechanics Symposium, ALASKA ROCKS 2005: Rock Mechanics for Energy, Mineral and Infrastructure Development in the Northern Regions, Anchorage*. 1–6. https://www.rocscience.com/assets/resources/learning/papers/The-Shear-Strength-Reduction-Method-for-the-Generalized-Hoek-Brown-Criterion.pdf

Hoek, E., Marinos, P., & Benissi, M. (1998). Applicability of the geological strength index (GSI) classification for very weak and sheared rock masses. The case of the Athens Schist Formation. *Bulletin of Engineering Geology and the Environment*, 57(2), 151–160. https://doi.org/10.1007/s100640050031

Hoek, E, Kaiser, P. K., & Bawden, W. F. (2000). *Support of Underground Excavations in Hard Rocks* (CRC Press (ed.)).

Hoek, Evert., Carranza-Torres, C., & Corkum, B. (2002). Hoek-Brown failure criterion-2002 Edition. *Proc. 5th North American Rock Mechanics Symposium and the 17th Tunnelling Association of Canada Conference, Toronto*. Vol. 1, 267–273. www.rocscience.com.

ISMR. (2015). The ISRM Suggested Methods for Rock Characterization, Testing and Monitoring: 2007-2014. En R. Ulusay (Ed.), *The ISRM Suggested Methods for Rock Characterization, Testing and Monitoring: 2007-2014*. Springer International Publishing. https://doi.org/10.1007/978-3-319-07713-0

Jordá-Bordehore, L., Martín-García, R., Alonso-Zarza, A., Jordá-Bordehore, R., & Romero-Crespo, P. (2016). *Stability assessment of shallow limestone caves through an empirical approach : application of the stability graph method to the Castañar Cave study site (Spain)*. https://doi.org/10.1007/s10064-015-0836-4

Marinos, V., & Carter, T. G. (2018). Maintaining geological reality in application of GSI for design of engineering structures in rock. *Engineering Geology*, 239, 282–297. https://doi.org/10.1016/j.enggeo.2018.03.022

Nadimi, S., Shahriar, K., Sharifzadeh, M., & Moarefvand, P. (2011). Triaxial creep tests and back analysis of time-dependent behavior of Siah Bisheh cavern by 3-Dimensional Distinct Element Method. *Tunnelling and Underground Space Technology*, 26(1), 155–162. https://doi.org/10.1016/j.tust.2010.09.002

Pandey, V. H. R., Kainthola, A., & Singh, T. N. (2022). *Empirical and Numerical Evaluation of a Cut Slope Near Rishikesh , India Empirical and Numerical Evaluation of a Cut Slope Near Rishikesh , India*. *June*. https://doi.org/10.1007/978-981-16-9770-8

Piccini, L., & Mecchia, M. (2009). Solution weathering rate and origin of karst landforms and caves in the quartzite of Auyan-tepui (Gran Sabana, Venezuela). *Geomorphology*, 106(1–2), 15–25. https://doi.org/10.1016/j.geomorph.2008.09.019

Rocscience. (2022). *RocLab* (4.0.0.1). https://www.rocscience.com/support/program-downloads

Sajid, M., & Arif, M. (2015). Reliance of physico-mechanical properties on petrographic characteristics: consequences from the study of Utla granites, north-west Pakistan. *Bulletin of Engineering Geology and the Environment*, 74(4), 1321–1330. https://doi.org/10.1007/s10064-014-0690-9

Sánchez Cortez, J. L. (2017). *Guía Espeleológica de Napo*.

Sánchez Cortez, J. L., Cárdenas Pinto, V., Ocampos Valarezo, D., Jaque Bonilla, D., Quilumba Dután, D., Ortiz Barrionuevo, J., Quinteros Cevallos, R., & Toledo Rojas, N. (2017). *Aplicación de Proceso Metodológico para el Inventario Geoturístico de Cavidades Naturales en la Provincia de Napo – Ecuador Application of Methodological Process for the Geotouristic Inventory of Natural Cavities in Napo Province - Ecuador*. 40, 61–73.

Sari, M. (2022). Two- and three-dimensional stability analysis of underground storage caverns in soft rock (Cappadocia, Turkey) by finite element method. *Journal of Mountain Science*, 19(4), 1182–1202. https://doi.org/10.1007/s11629-021-7047-1

Shalabi, F. I., Al-Qablan, H. A., & Al-Hattamleh, O. H. (2009). Elasto-plastic behavior of raghadan tunnel based on RMR and hoek - Brown classifications. *Geotechnical and Geological Engineering*, 27(2), 237–248. https://doi.org/10.1007/s10706-008-9225-0

Singh, A. K., Sinha, S. K., & Paul, A. (2019). *Variation of RMR for different rock types as immediate roof in Jharia Coalfield of India*. *July*.

Spyridis, P., Fortsakis, P., & Schwind, T. (2018). Geotechnical Engineering and Innovative Support System for Shallow Urban Subway Caverns in Rock, in Confined Built Environment. *Geotechnical and Geological Engineering*, 36(5), 2967–2983. https://doi.org/10.1007/s10706-018-0516-9

Sumner, P., & Nel, W. (2002). The effect of rock moisture on Schmidt hammer rebound: Tests on rock samples from Marion Island and South Africa. *Earth Surface Processes and Landforms*, 27(10), 1137–1142. https://doi.org/10.1002/esp.402

Vallejo, C., Hochuli, P. A., Winkler, W., & von Salis, K. (2002). Palynological and sequence stratigraphic analysis of the Napo Group in the Pungarayacu 30 well, Sub-Andean Zone, Ecuador. *Cretaceous Research*, 23(6), 845–859. https://doi.org/10.1006/cres.2002.1028

Van Kien, D., Anh, D. N., & Thai, D. N. (2022). Numerical Simulation of the Stability of Rock Mass around Large Underground Cavern. *Civil Engineering Journal*, 8(1), 81–91. https://doi.org/10.28991/CEJ-2022-08-01-06

Vásárhelyi, B., & Kovács, D. (2017). Empirical methods of calculating the mechanical parameters of the rock mass. *Periodica Polytechnica Civil Engineering*, 61(1), 39–50. https://doi.org/10.3311/PPci.10095

Vassilis, M. (2020). Applications of the GSI System to the Classification of Soft Rocks. En *Soft Rock Mechanics and Engineering* (pp. 503–539). Springer. https://doi.org/10.1007/978-3-030-29477-9_19

Vera, D., Simbaña-Tasiguano, M., Guzmán, O., Cabascango, E., Sánchez-Cortez, J. L., Campos, C., & Grefa, H. (2023). Quantitative Assessment of Geodiversity in Ecuadorian Amazon—Case Study: Napo Sumaco Aspiring UNESCO Geopark. *Geoheritage*, 15(1), 1–14. https://doi.org/10.1007/s12371-023-00792-2

Waltham, A. C., & Fookes, P. G. (2005). Engineering classification of karst ground conditions. *Quarterly Journal of Engineering Geology and Hydrogeology*, 36(2), 101–118. https://doi.org/10.1144/1470-9236/2002-33

Yépez, S., Ocampos, A., Espín, J., & Chulde, E. (2022). Geomechanical Evaluation of the Stability of the Humanti caverns, Archidona-Napo. *GEOLatitud*, 5(2), 14–27.

APPENDIX

Input Parameters to Determinate the Geological Strenght Index

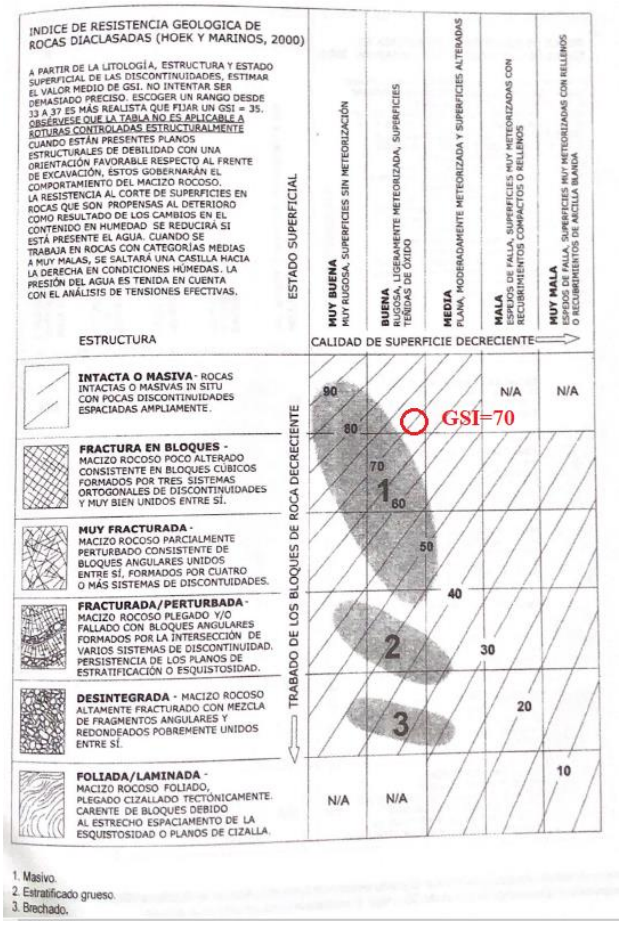

Figure A1: Valor de GSI para la Caliza Fosilífera.
Source: Marinos and Carter, 2018

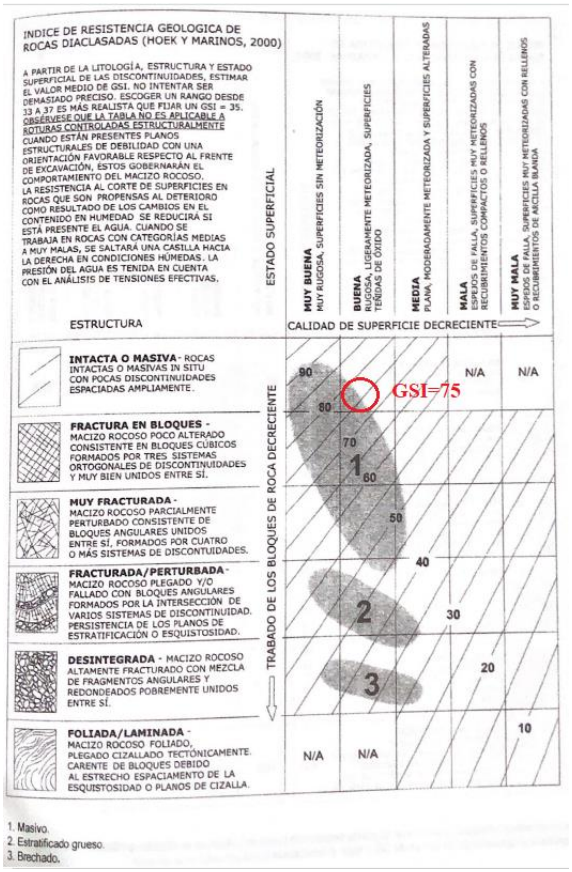

Figure A2: Valor de GSI para la Caliza Masiva.
Source: Marinos and Carter, 2018

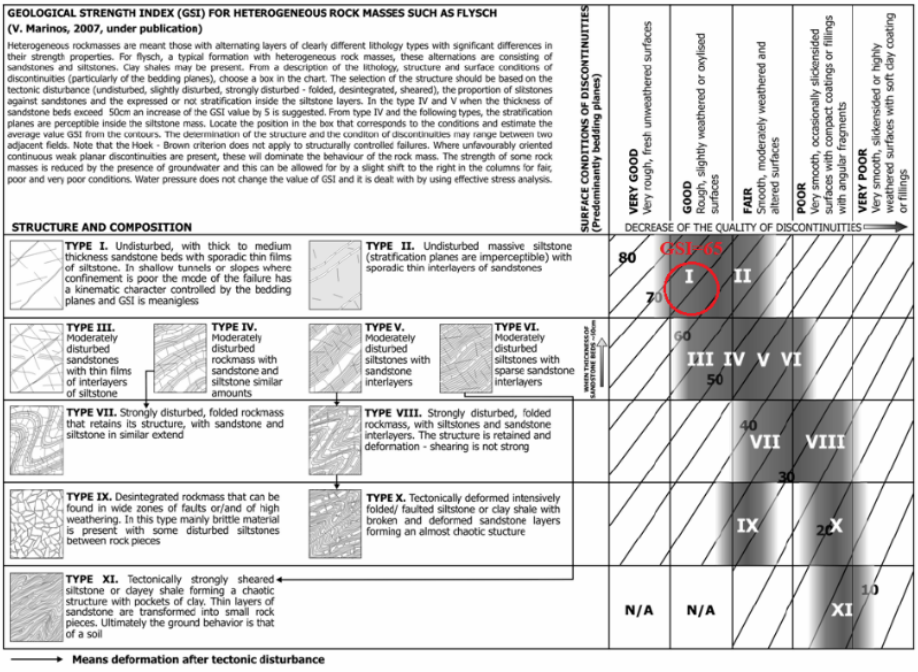

Figure A3: Valor de GSI para las Lutitas.
Source: Marinos and Carter, 2018

RocLab Parameters

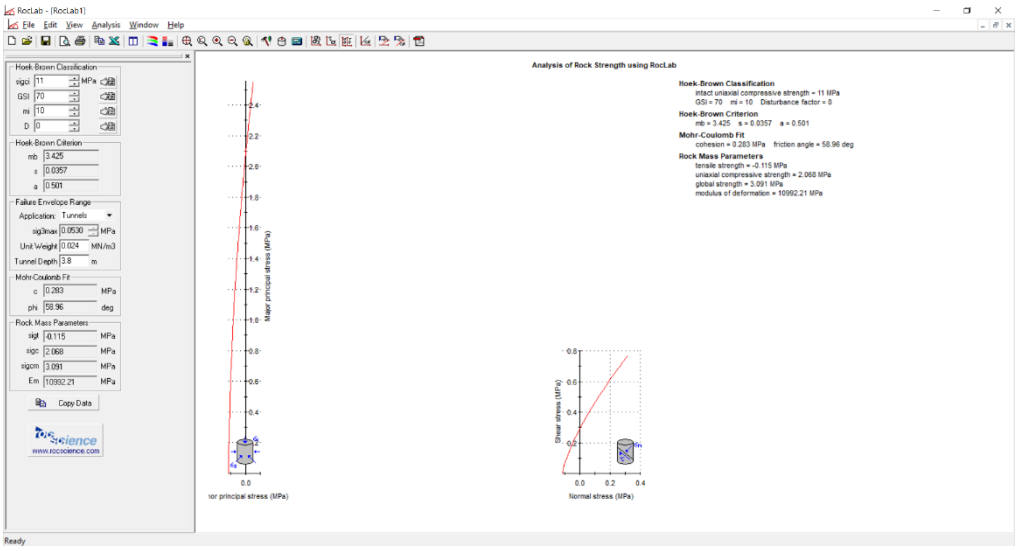

Figure A4: Caliza Fosilífera
Source: Rocscience, 2022

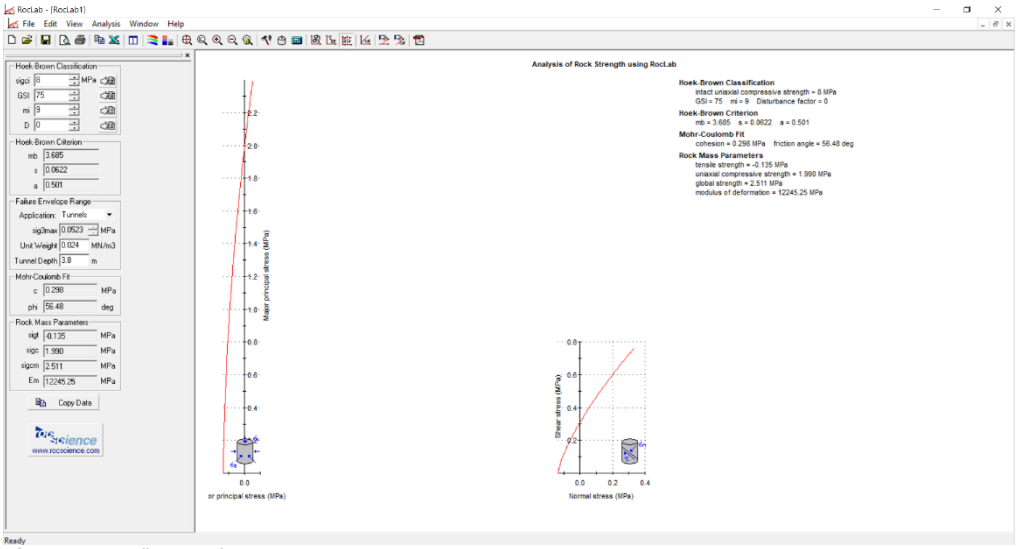

Figure A5: Caliza Masiva
Source: Rocscience, 2022

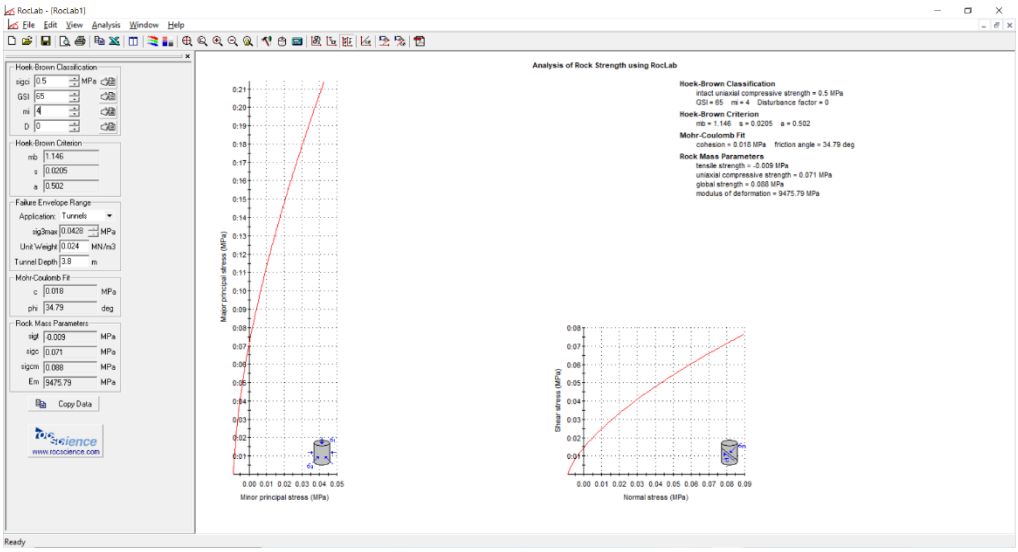

Figure A6: adShale
Source: Rocscience, 2022